FK228 and oncogenic H-Ras synergistically induce Mek1/2 and Nox-1 to generate reactive oxygen species for differential cell death

Shambhunath Choudhary[a], Kusum Rathore[a,b] and Hwa-Chain Robert Wang[a,b]

To investigate the mechanism behind the pro-apoptotic ability of oncogenic H-Ras to enhance FK228-induced apoptosis, we primarily used the 10T1/2-TR-H-*Ras* cell line, in which ectopic expression of oncogenic H-Ras(V12) is controlled by the addition of tetracycline into cultures, and secondarily used oncogenic H-Ras-expressing MCF10A cells in our studies. Our results showed the pro-apoptotic roles of Mek1/2 activation, nicotinamide adenine dinucleotide phosphate-oxidase 1 (Nox-1) elevation, and reactive oxygen species (ROS) production in FK228-induced selective cell death of oncogenic H-Ras-expressing cells versus counterpart cells. We found that although Nox-1 elevation and ROS production played essential roles in oncogenic H-Ras-induced cell proliferation and morphological transformation, the expression of oncogenic H-Ras and FK228 treatment synergistically induced activation of Mek1/2. This activation resulted in differentially increased Nox-1 elevation and ROS production leading to selective cell death of oncogenic H-Ras-expressing cells versus counterpart cells. We also found that FK228 treatment induced mitochondrial ROS and Mek1/2 activation, bypassing Raf-1, to downstream Erk1/2, participating in the induction of selective cell death. Thus, the pro-apoptotic abilities of Mek1/2 and Nox-1 should be considered as potential targets in designing therapeutic protocols using FK228 to assure ROS-mediated cell death for treating cancer cells acquiring Ras activation. *Anti-Cancer Drugs* 21:831–840 © 2010 Wolters Kluwer Health | Lippincott Williams & Wilkins.

Anti-Cancer Drugs 2010, **21**:831–840

Keywords: FK228, Nox-1, oncogenic Ras, reactive oxygen species, selective cell death

[a]Anticancer Molecular Oncology Laboratory, Department of Comparative Medicine, College of Veterinary Medicine and [b]Graduate School of Genome Science and Technology, The University of Tennessee, Knoxville, Tennessee, USA

Correspondence to Dr Hwa-Chain Robert Wang, DVM, PhD, Department of Comparative Medicine, College of Veterinary Medicine, 2407 River Drive, The University of Tennessee, Knoxville, TN 37996, USA
Tel: +1 865 974 3846; fax: +1 865 974 5640; e-mail: hcrwang@utk.edu

Received 24 June 2010 **Revised form accepted** 5 July 2010

Introduction

Oncogenic activation of *Ras* genes is widely involved in human cancers [1]. In our earlier studies, we showed that the expression of oncogenic H-Ras(V12) in human urinary bladder cancer J82, human colorectal cancer HT29, and mouse embryo fibroblast 10T1/2 cells not only results in cellular acquisition of tumorigenicity, mimicking the acquisition of oncogenic activation of the H-*Ras* gene in tumor progression, but also increases the susceptibility of oncogenic H-Ras-expressing cells to the histone deacetylase inhibitors (HDACIs) FK228 and trichostatin A for inducing apoptosis. These results suggest a pro-apoptotic ability of oncogenic H-Ras to facilitate HDACI-induced apoptosis in addition to its well-known transforming ability [2–5]. FK228 selectively inhibits class I HDACIs and exhibits pleiotropic anti-tumor activities [6]. We presented evidence that differential regulations of the ERK (extracellular signal-regulated kinase) pathway, the p38/stress activated protein kinase pathway, core histone acetylation, $p21^{Cip1}$ and $p27^{Kip1}$ expression, and the caspase pathways contribute to FK228-induced selective apoptosis of oncogenic H-Ras-expressing cells versus their counterpart cells [2–5]. Recently, we reported that differentially elevated, intracellular reactive oxygen species (ROS) play an important role in the pro-apoptotic ability of oncogenic H-Ras to enhance FK228-induced apoptosis; FK228 treatment results in the differential elevation of ROS for inducing selective apoptosis in oncogenic H-Ras-expressing, J82-Ras, and HT29-Ras cells versus their counterpart J82 and HT29 cells, respectively [7]. However, the mechanism for the ROS-mediated, pro-apoptotic ability of H-Ras to enhance FK228-induced apoptosis remains to be determined.

Targeting cancer cells by ROS-mediated mechanisms is a new approach under serious investigation to develop effective, therapeutic strategies for disease control. Expression of oncogenic H-Ras has been shown to elevate intracellular ROS through the ERK pathway to upregulate nicotinamide adenine dinucleotide phosphate-oxidase-1 (Nox-1) gene expression [8,9]. Nox-1 generates intracellular ROS, and increased Nox-1 expression is seen in various human cancers [10]. However, whether Nox-1 is modulated by oncogenic H-Ras and FK228 to induce profound ROS production, leading to accelerated apoptosis, remains to be clarified.

In this paper, we used the 10T1/2-TR-H-*Ras* cell line [5], in which ectopic expression of oncogenic H-Ras(V12) is controlled by the addition of tetracycline (Tet) into

0959-4973 © 2010 Wolters Kluwer Health | Lippincott Williams & Wilkins DOI: 10.1097/CAD.0b013e32833ddba6

Copyright © Lippincott Williams & Wilkins. Unauthorized reproduction of this article is prohibited.

cultures, to show the pro-apoptotic roles of Mek1/2 activation, Nox-1 elevation, and ROS production in FK228-induced selective death of oncogenic H-Ras-expressing cells versus counterpart cells. We also used the noncancerous human breast epithelial MCF10A cell line to develop oncogenic H-Ras-expressing, MCF10A-Ras cell lines to verify our findings in 10T1/2-TR-H-*Ras* cells.

Materials and methods

Cell cultures and reagents

10T1/2-TR-H-*Ras* cells were maintained in Basal Medium Eagle supplemented with 10% fetal bovine serum, 100 U/ml penicillin, and 100 μg/ml streptomycin in 5% CO_2 at 37°C [5]. Human breast epithelial cell line MCF10A (American Type Culture Collection, Rockville, Maryland, USA) and its derived cell lines were maintained in a complete MCF10A culture medium (1 : 1 mixture of Dulbecco's modified Eagle's medium and Ham's F12, supplemented with 100 ng/ml cholera enterotoxin, 10 μg/ml insulin, 0.5 μg/ml hydrocortisol, 20 ng/ml epidermal growth factor, and 5% horse serum) [11]. Stock aqueous solutions of FK228 (National Cancer Institute, Chemistry and Synthesis Branch, collaboration with Dr K.K. Chan, The Ohio State University, Ohio, USA), chloromethyl-dichlorodihydrofluorescein-diacetate (Invitrogen/Molecular Probes, Carlsbad, California, USA), rhodamine-123 (Rho-123), rotenone (ROT) (Sigma–Aldrich, St Louis, Missouri, USA), U0126 (Cell Signaling Technology, Beverly, Massachusetts, USA) and diphenylene iodonium [(DPI), Acros, Morris Plains, New Jersey, USA], were prepared in dimethyl sulfoxide and diluted in a culture medium for the assays. A stock aqueous solution of *N*-acetyl-L-cysteine (NAC) (Alexis, San Diego, California, USA) was prepared in distilled water and diluted in culture media for assays.

Cell proliferation assay

Cell proliferation was determined using the 5-bromo-2′-deoxyuridine (BrdU) cell proliferation enzyme-linked immunosorbent assays (ELISA) kit (Roche, Indianapolis, Indiana, USA) [2,3]. A number of cells (5×10^4) were seeded into each well of 96-well culture plates. After the indicated treatments, the cells were labeled with BrdU for 12 h, fixed, incubated with peroxidase-conjugated BrdU-specific antibodies, and stained with the peroxidase substrate. Quantification of BrdU-labeled cells was determined with an ELISA reader (Bio-Tek, Winooski, Vermont, USA).

Cell viability assay

A methyl thiazolyl tetrazolium (MTT) assay kit (ATCC, Manassas, Virginia, USA) was used to measure cell viability [2,3]. Cells (5×10^4) were seeded into each well of 96-well culture plates for 24 h. After indicated treatments, cells were incubated with MTT reagent for 4 h, and then with a detergent reagent for 24 h. A reduced MTT reagent in cultures was quantified with an ELISA reader (Bio-Tek).

Annexin-V apoptosis assay

An annexin-V-fluorescein isothiocyanate (FITC) apoptosis detection kit with propidium iodide (BD Biosciences, San Jose, California, USA) was used to detect apoptotic cell death by flow cytometry [2,3]. In brief, cells were collected after trypsinization and washed with PBS. The cells were then incubated with annexin V-FITC and propidium iodide in a binding buffer (10 mmol/l HEPES–KOH, pH 7.4, 150 mmol/l NaCl, 1.8 mmol/l $CaCl_2$) for 20 min at ambient temperature in the dark. Flow cytometric analysis was done using the Coulter EPICS Elite Cytometer (Hialeah, Florida, USA) at the excitation and emission wavelengths of 488 and 550 nm, respectively, for FITC measurements, and at 488 and 645 nm for propidium iodide measurements. Both subpopulations of annexin V-FITC-labeled cells and propidium iodide-labeled cells were considered together to determine the percentage of cells undergoing apoptotic cell death using Multicycle software (Phoenix Flow System, San Diego, California, USA).

Measurement of intracellular reactive oxygen species

The cells were incubated with 5 μmol/l chloromethyl-dichlorodihydrofluorescein-diacetate in 5% CO_2 at 37°C for 1 h [12]. They were trypsinized and resuspended in PBS for flow cytometry analysis using a 15 mw air-cooled argon laser to produce 488 nm light. Dichlorofluorescein fluorescence emission was collected with a 529-nm band pass filter [7]. The mean fluorescence intensity of 2×10^4 cells was quantified using Multicycle software (Phoenix Flow System).

Measurement of mitochondrial membrane potential ($\Delta\psi m$)

To measure mitochondrial membrane potential, the cells were incubated with 1 μmol/l Rho-123 in 5% CO_2 at 37°C for 1 h [12]. They were rinsed with PBS, trypsinized from cultures, and resuspended in PBS for flow cytometric analysis, as described above, at the excitation and emission wavelengths of 488 and 529 nm, respectively, for Rho-123 fluorescence measurements.

Measurement of glutathione

Total intracellular glutathione (GSH) levels were measured with a GSH assay kit (Cayman Chemical, Ann Arbor, Michigan, USA). In brief, the cells were sonicated in an ice-cold buffer (50 mmol/l K_2HPO_4, 1 mmol/l EDTA, pH 7); cell lysates were isolated from the supernatants after centrifugation at 10 000 × g for 15 min at 4°C and deproteinated in 10% metaphosphoric acid (Sigma–Aldrich). Protein concentration in cell lysates was measured using the bicinchoninic acid (BCA) assay (Pierce, Rockford, Illinois, USA). Deproteinated cell lysates (50 μl) were incubated with 150 μl reaction buffer (0.4 mol/l 2-(*N*-morpholino)ethanesulfonic acid, 0.1 mol/l phosphate, pH 6.0, 2 mmol/l EDTA, 0.24 mmol/l nicotinamide adenine dinucleotide phosphate-oxidase, 0.1 mmol/l 5,5′-dithiobis

Copyright © Lippincott Williams & Wilkins. Unauthorized reproduction of this article is prohibited.

Fig. 1

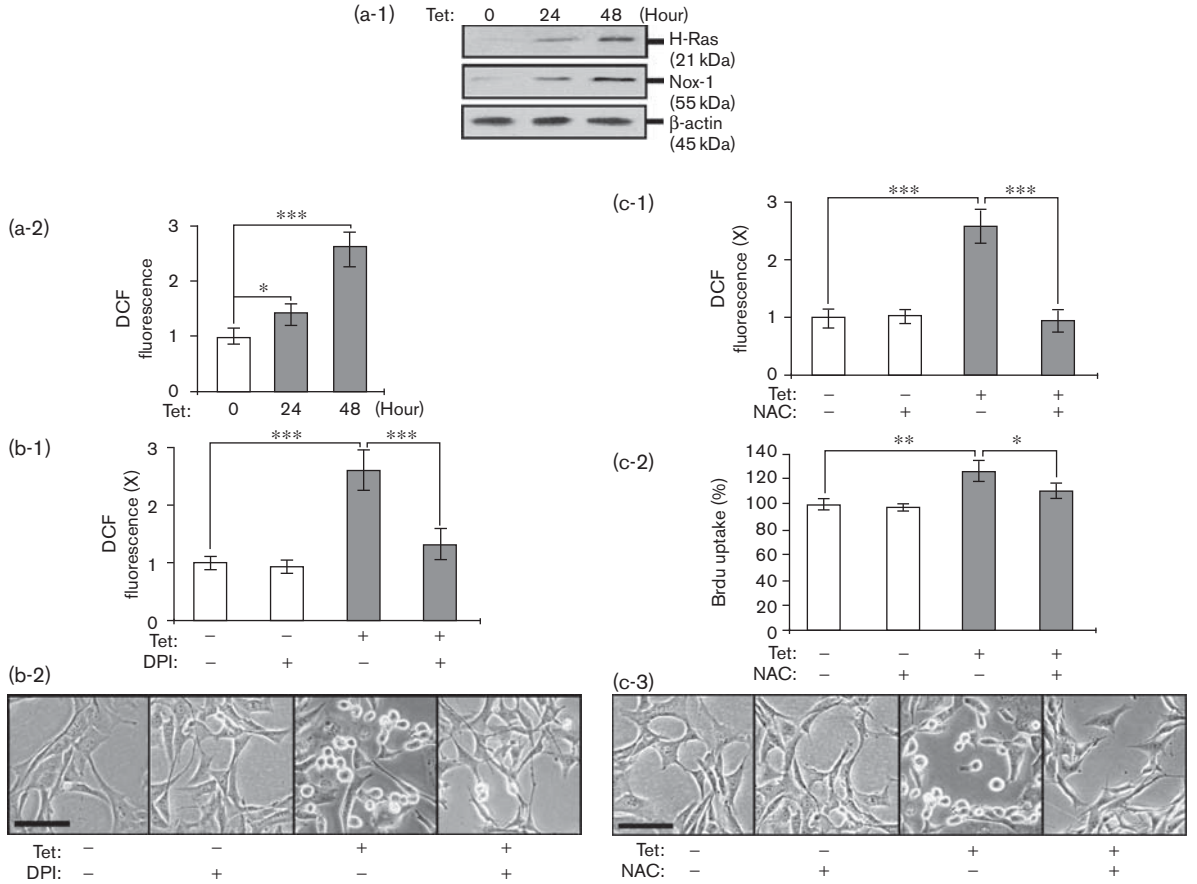

Nicotinamide adenine dinucleotide phosphate-oxidase-1 (Nox-1) and reactive oxygen species (ROS) induction by oncogenic H-Ras in 10T1/2 cells. 10T1/2-TR-H-*Ras* cells were induced with 100 ng/ml tetracycline (Tet) to express oncogenic H-Ras (a-1 and a-2) in the presence or absence of 0.1 μmol/l diphenylene iodonium (DPI) (b-1 and b-2) or 5 mmol/l *N*-acetyl-L-cysteine (NAC) (c-1–c-3) for 48 h. (a-1) Cell lysates were analyzed by western immunoblotting to detect H-Ras and Nox-1, with β-actin as a control. (a-2, b-1, and c-1) ROS levels were measured with CM-H_2DCF-DA labeling; relative level of ROS, as fold induction (X, arbitrary unit), was normalized by the level determined in the uninduced, untreated counterpart cells, set as 1. (b-2 and c-3) Morphological features of cells. Images were acquired at × 20 objective magnification. Bar indicates 100 μm. (c-2) Cell proliferation was determined; relative cell growth rate was normalized by the value of 5-bromo-2′-deoxyuridine (BrdU) found in uninduced, untreated cells, set as 100%. Columns, mean of triplicates (a-2, b-1, and c-1) or tetraplicates (c-2); bars, standard deviation. The Student's *t*-test was used to analyze statistical significance, indicated by $*P<0.05$, $**P<0.01$, $***P<0.001$. All results are representative of three independent experiments. DCF, dichlorofluorescein.

(2-nitrobenzoic acid), and 0.1 unit glutathione reductase) at 37°C for 30 min. Total GSH was determined by absorbance at 405 nm using GSH disulfide as a standard. Each sample was assessed in duplicate and the levels were expressed as GSH per milligram cell lysate protein.

Western immunoblotting

The cells were lysed in buffer A (10 mmol/l Tris–HCl, 150 mmol/l NaCl, 1% Triton X-100, 5 mmol/l EDTA, 10 mmol/l sodium pyrophosphate, 10% glycerol, 0.1% Na_3VO_4, and 50 mmol/l NaF, pH 7.4) [2–5], followed by centrifugation at 20 000 × g for 20 min to isolate cell lysates from the supernatants. Protein concentration in cell lysates was measured using the BCA assay (Pierce). Aliquots of cellular proteins were resolved by electrophoresis in 10% SDS-polyacrylamide gels and transferred to nitrocellulose filters for western immunoblotting as described earlier [2–5]. Antibodies specific to H-Ras (21 kDa), Raf-1 (74 kDa), Erk1/2 (44/42 kDa), Nox-1 (55 kDa), and β-actin (45 kDa) were purchased from Santa Cruz Biotechnology (Santa Cruz, California, USA). Antibodies specific to Mek1/2 (45 kDa) and phosphorylated forms of Raf-1 (p-Raf-1), Mek1/2 (p-Mek1/2), and Erk1/2 (p-Erk1/2) were purchased from Cell Signaling Technology. Antigen–antibody complexes on filters were found by the Supersignal chemiluminescence kit (Pierce).

Caspase activity assay

Caspase-3/7 activity was measured using a Caspase-Glo assay kit (Promega, Madison, Wisconsin, USA). Cells were lysed in buffer A [2,3], followed by centrifugation at 20 000 × g for 20 min to isolate cell lysates from the

Copyright © Lippincott Williams & Wilkins. Unauthorized reproduction of this article is prohibited.

Fig. 2

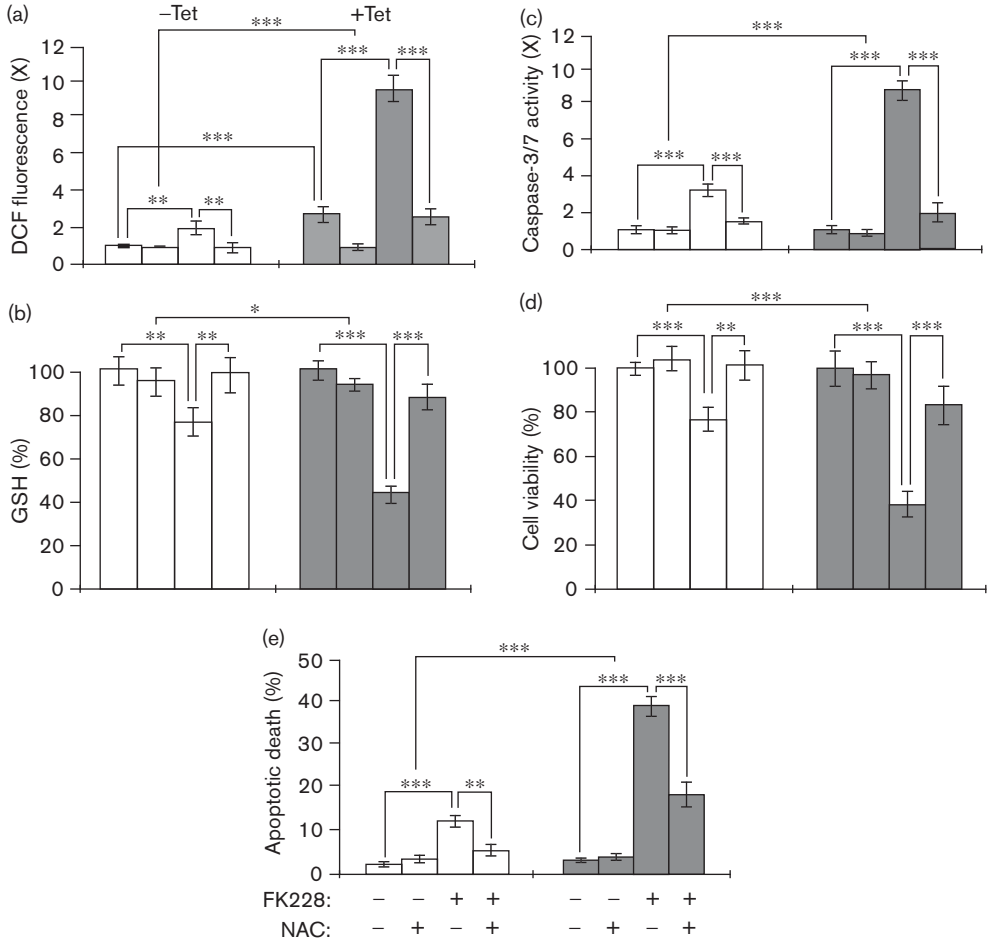

Reactive oxygen species-mediated apoptosis and glutathione (GSH) depletion induced by FK228 in 10T1/2 cells. 10T1/2-TR-H-*R*as cells [no tetracycline (–Tet), white columns] were induced with 100 ng/ml tetracycline (Tet) to express oncogenic H-Ras [with tetracycline (+Tet), dark columns] in the presence or absence of 1 nmol/l FK228 and 5 mmol/l *N*-acetyl-L-cysteine (NAC) for 48 h. (a) Reactive oxygen species levels were measured; relative level, as fold induction (X, arbitrary unit), was normalized by the level determined in the uninduced, untreated counterpart cells, set as 1. (b) GSH content was determined; relative GSH level was normalized by the value determined in untreated counterpart cells, set as 100%. (c) The activity of caspase-3/7 was measured; relative caspase activity, as fold induction (X, arbitrary unit), was normalized by the values determined in the untreated counterpart cells, set as 1. (d) Cell viability was measured; relative cell viability was normalized by the value determined in untreated counterpart cells, set as 100%. (e) Apoptotic cell population (%) was measured by flow cytometry with an Annexin-V-fluorescein isothiocyanate apoptosis detection kit. Columns, mean of triplicates (a, b, c, and e) or tetraplicates (d); bars, standard deviation. The Student's *t*-test was used to analyze statistical significance, indicated by $*P<0.05$, $**P<0.01$, $***P<0.001$. All results are representative of three independent experiments. DCF, dichlorofluorescein.

supernatants. Protein concentrations in cell lysates were measured using the BCA assay (Pierce). Protein (30 μg) was incubated with a proluminescent substrate specific for caspase-3/7 in white-walled, 384-well plates at ambient temperature for 1 h; the released luminescence was measured in a luminometer plate reader (Bio-Tek).

Statistical analysis

The Student's *t*-test was used to analyze statistical significance, indicated by $*P<0.05$, $**P<0.01$, $***P<0.001$; a P value of less than or equal to 0.05 was considered significant.

Results and discussion

Nox-1 mediated, H-Ras-induced reactive oxygen species in 10T1/2 cells

To verify the association of ROS production with oncogenic H-Ras expression in 10T1/2-TR-H-Ras cells, we treated cells with Tet to induce ectopic expression of oncogenic H-Ras. We found that Tet treatment resulted in increased H-Ras expression in a time-dependent manner (Fig. 1a-1); Nox-1 (Fig. 1a-1) and ROS (Fig. 1a-2) levels were elevated in concert with the increased levels of H-Ras. To verify the role of Nox-1 in H-Ras-induced ROS generation, we used the flavoprotein inhibitor DPI [13] to block Nox-1 activity. We found that DPI treatment effectively blocked the

Copyright © Lippincott Williams & Wilkins. Unauthorized reproduction of this article is prohibited.

Fig. 3

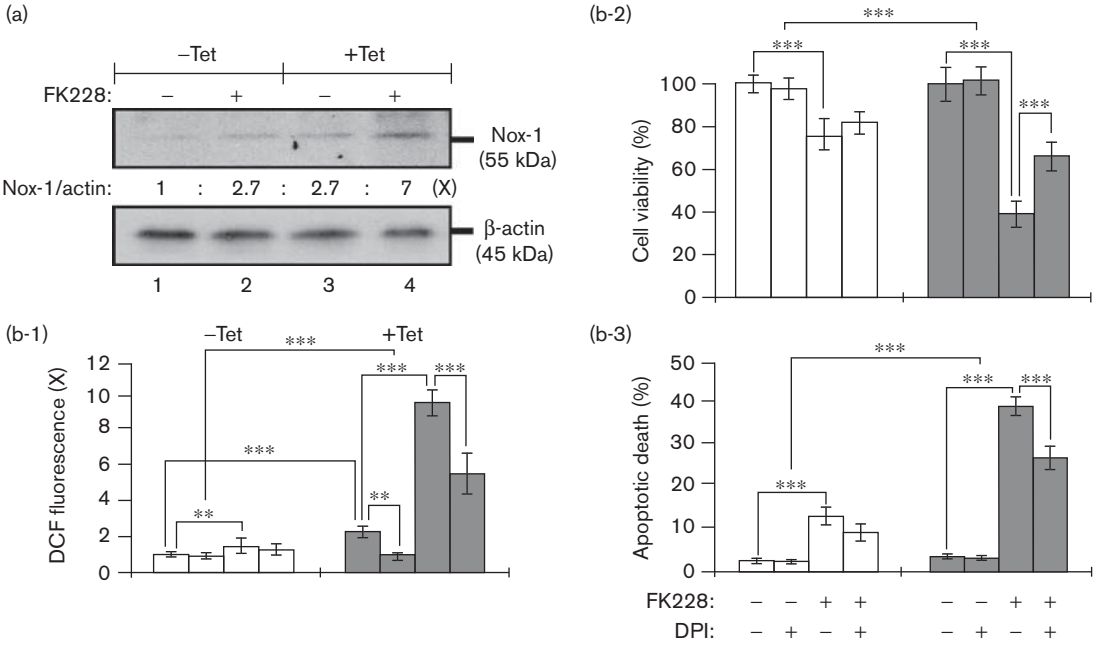

Nicotinamide adenine dinucleotide phosphate-oxidase 1 (Nox-1) in FK228-induced apoptosis of 10T1/2 cells. 10T1/2-TR-H-*R*as cells [no tetracycline (–Tet), white columns] were induced with 100 ng/ml tetracycline (Tet) to express oncogenic H-Ras [with tetracycline (+Tet), dark columns] in the presence or absence of 1 nmol/l FK228 (a, b-1–b-3) and 0.1 μmol/l diphenylene iodonium (DPI) (b-1–b-3) for 48 h. (a) Cell lysates were analyzed by western immunoblotting to detect Nox-1, with β-actin as a control. Levels of Nox-1 and β-actin were quantified by densitometry. The relative levels of Nox-1 (Nox-1/actin) were calculated by normalizing the levels of Nox-1 with the levels of β-actin, and then were normalized by the level in uninduced, untreated cells (lane 1), set as 1 (X, arbitrary unit). (b-1) Reactive oxygen species levels were measured; relative level, as fold induction (X, arbitrary unit), was normalized by the level determined in the uninduced, untreated counterpart cells, set as 1. (b-2) Cell viability was measured; relative cell viability was normalized by the value determined in untreated counterpart cells, set as 100%. (b-3) Apoptotic cell population (%) was measured by flow cytometry with an Annexin-V-fluorescein isothiocyanate apoptosis detection kit. Columns, mean of triplicates (b-1 and b-3) or tetraplicates (b-2); bars, standard deviation. The Student's *t*-test was used to analyze statistical significance, indicated by $^{**}P<0.01$, $^{***}P<0.001$. All results are representative of three independent experiments. DCF, dichlorofluorescein.

Tet-induced, H-Ras-induced ROS elevation (Fig. 1b-1) and morphological changes from normal spindle morphology to transformed, rounded, refractile morphology (Fig. 1b-2). In addition, we found that the general antioxidant NAC [12,14] effectively blocked H-Ras-induced ROS production (Fig. 1c-1), cell proliferation (Fig. 1c-2), and morphological changes (Fig. 1c-3). These results verified that Nox-1 elevation and ROS production played essential roles in oncogenic H-Ras-induced cell proliferation and morphological transformation in 10T1/2-TR-H-Ras cells.

Differentially reactive oxygen species-mediated apoptosis of 10T1/2 cells

We showed that differential ROS production plays an important role in FK228-induced differential activation of caspases and selective apoptosis of H-Ras-expressing, human urinary bladder cancer J82 cells [7]. To verify the association of FK228-induced differential activation of caspases and selective apoptosis with H-Ras-increased ROS production in 10T1/2-TR-H-*Ras* cells, we treated cells with Tet and FK228, and blocked ROS production with NAC. We found that H-Ras expression and FK228 treatment resulted in a synergistic increase in ROS production, and NAC treatment effectively blocked FK228-increased ROS production (Fig. 2a). We also found that FK228 treatment resulted in GSH reduction (Fig. 2b), activation of caspases (Fig. 2c), reduction of cell viability (Fig. 2d), and induction of apoptotic cell death (Fig. 2e). NAC treatment effectively reversed FK228-induced reduction of GSH, activation of caspases, reduction of cell viability, and apoptotic cell death. GSH represents an important ROS-scavenging system required to inactivate intracellular ROS [15], and depletion of GSH increases cell sensitivity to ROS for inducing apoptosis [16]. Our results showed that reduction of GSH, activation of caspases, reduction of cell viability, and induction of apoptotic cell death were highly correlated with increased levels of ROS induced by FK228. Thus, differential ROS production played an important role in differential activation of caspases, GSH reduction, and apoptotic cell death induced by FK228 in a Ras-dependent manner.

Nox-1 mediated reactive oxygen species in FK228-induced apoptosis of 10T1/2 cells

Investigating whether Nox-1 was involved in FK228-induced ROS production, we found that FK228 treatment

Copyright © Lippincott Williams & Wilkins. Unauthorized reproduction of this article is prohibited.

Fig. 4

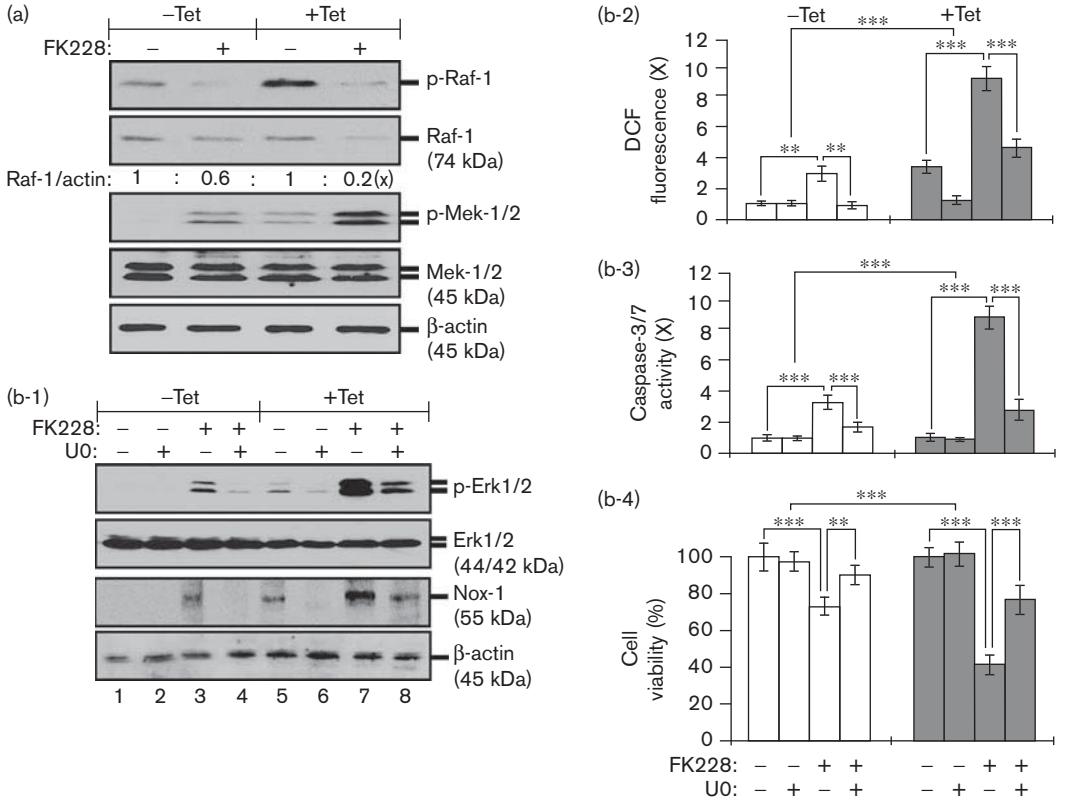

The ERK pathway mediated H-Ras-induced and FK228-induced reactive oxygen species, Nicotinamide adenine dinucleotide phosphate-oxidase 1 (Nox-1), and death in 10T1/2 cells. 10T1/2-TR-H-*R*as cells [no tetracycline (–Tet), white columns] were induced with 100 ng/ml tetracycline (Tet) to express oncogenic H-Ras [with tetracycline (+Tet), dark columns] in the presence or absence of 1 nmol/l FK228 (a, b-1 to b-4) and 10 μmol/l U0126 (U0) (b-1–b-4) for 48 h. (a and b-1) Cell lysates were analyzed by western immunoblotting to detect p-Raf-1, Raf-1, p-Mek1/2, Mek1/2, p-Erk1/2, Erk1/2, and Nox-1 with β-actin as a control. (a) Levels of Raf-1 and β-actin were quantified by densitometry. The relative protein levels of Raf-1 (Raf-1/actin) were calculated by normalizing the levels of Raf-1 with the levels of β-actin, and then were normalized by the level in untreated cells (lane 1), set as 1 (X, arbitrary unit). (b-2) ROS levels were measured; relative level, as fold induction (X, arbitrary unit), was normalized by the level determined in the uninduced, untreated counterpart cells, set as 1. (b-3) The activity of caspase-3/7 was measured; relative caspase activity, as fold induction (X, arbitrary unit), was normalized by the value determined in untreated counterpart cells, set as 1. (b-4) Cell viability was determined; relative cell viability was normalized by the value determined in untreated counterpart cells, set as 100%. Columns, mean of triplicates (b-2 and b-3) or tetraplicates (b-4); bars, standard deiation. The Student's *t*-test was used to analyze statistical significance, indicated by $^{**}P<0.01$, $^{***}P<0.001$. All results are representative of three independent experiments. DCF, dichlorofluorescein.

resulted in Nox-1 elevation in 10T1/2-TR-H-*Ras* cells (Fig. 3a, lanes 2 and 4). Nox-1 level was increased by FK228 to a higher level in cells expressing oncogenic H-Ras (lane 4) than in counterpart cells (lane 2), and H-Ras expression and FK228 treatment resulted in synergistically increasing Nox-1 level (lane 4 vs. lanes 2 and 3). H-Ras expression and FK228 treatment also resulted in a synergistic increase of ROS level (Fig. 3b-1), reduction of cell viability (Fig. 3b-2), and induction of apoptotic cell death (Fig. 3b-3). Blockage of Nox-1 by DPI significantly reduced FK228-induced ROS production (Fig. 3b-1), reduction of cell viability (Fig. 3b-2), and apoptotic cell death (Fig. 3b-3) in cells expressing oncogenic H-Ras, and DPI treatment induced a modest reduction of FK228-induced ROS production and cell death in counterpart cells. Thus, differentially increased Nox-1 played a pro-apoptotic role in FK228-induced differential ROS elevation and cell death in oncogenic H-Ras-expressing cells versus counterpart cells. As an outcome, oncogenic H-Ras expression and FK228 treatment synergistically induced Nox-1 elevation, resulting in significant ROS production leading to selective cell death of oncogenic H-Ras-expressing cells versus counterpart cells.

The ERK pathway in H-Ras-induced and FK228-induced Nox-1, reactive oxygen species, and cell death in 10T1/2 cells

The ERK pathway mediates signals from Ras to induce Nox-1 for ROS production [9], and the ERK pathway is reportedly involved in ROS-mediated apoptosis induced by some anticancer agents [17]. Investigating the ERK pathway members involved in FK228-induced cell death, we found that FK228 treatment resulted in reducing phosphorylated Raf-1 and cognate Raf-1 protein but

Copyright © Lippincott Williams & Wilkins. Unauthorized reproduction of this article is prohibited.

Fig. 5

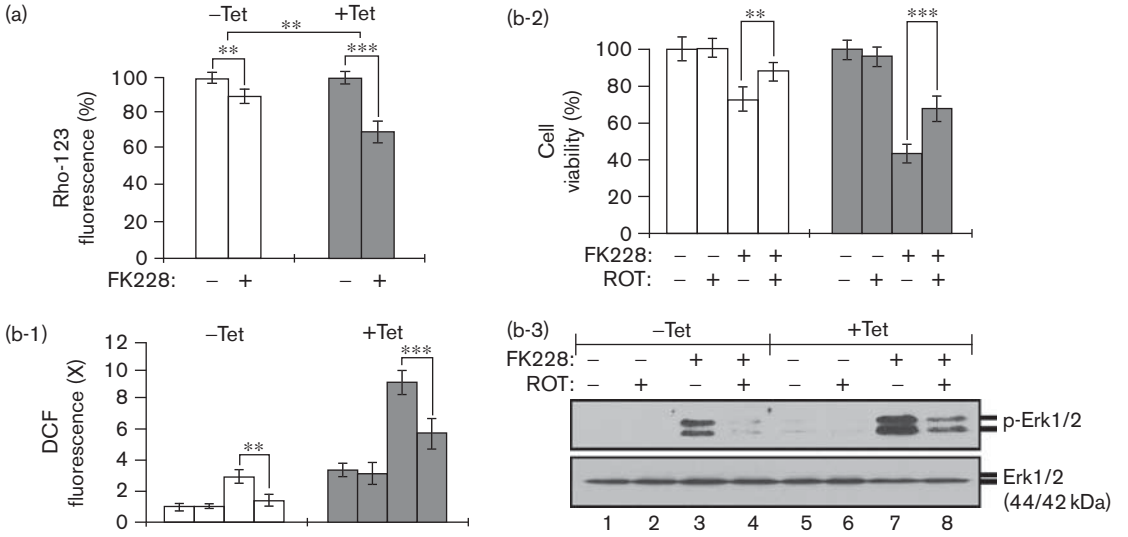

Induction of the ERK pathway by FK228-induced mitochondrial reactive oxygen species (ROS) in 10T1/2 cells. 10T1/2-TR-H-*R*as cells [no tetracycline (–Tet), white columns] were induced with 100 ng/ml tetracycline (Tet) to express oncogenic H-Ras [with tetracycline (+Tet), dark columns] in the presence or absence of 1 nmol/l FK228 (a, b-1–b-3) and 0.5 μmol/l rotenone (ROT) (b-1–b-3) for 48 h. (a) Cultures were then labeled with rhodamine-123 (Rho-123) for flow cytometric analysis of mitochondrial membrane potential. Relative fluorescence intensities in FK228-treated cultures were normalized by the fluorescence intensities determined in the untreated counterpart cells, set as 100%. (b-1) ROS levels were measured; relative level, as fold induction (X, arbitrary unit), was normalized by the level determined in the uninduced, untreated counterpart cells, set as 1. (b-2) Cell viability was determined; relative cell viability was normalized by the value determined in untreated counterpart cells, set as 100%. (b-3) Cell lysates were analyzed by western immunoblotting to detect p-Erk1/2 and Erk1/2. Columns, mean of triplicates (a and b-1) or tetraplicates (b-2); bars, standard deviation. The Student's *t*-test was used to analyze statistical significance, indicated by $^{**}P<0.01$, $^{***}P<0.001$. All results are representative of three independent experiments. DCF, dichlorofluorescein.

increasing Mek1/2 phosphorylation (Fig. 4a). Using the Mek1/2-specific inhibitor, U0126 [5], to block the downstream ERK pathway, we found that H-Ras expression induced the ERK pathway indexed by Erk1/2 phosphorylation (Fig. 4b-1, lane 5 vs. lane 1). FK228 treatment enhanced Erk1/2 phosphorylation (lanes 3 and 7 vs. lanes 1 and 5, respectively), and U0126 treatment reduced FK228-induced and H-Ras-induced Erk1/2 phosphorylation and Nox-1 elevation (lanes 4, 6, and 8 vs. lanes 3, 5, and 7, respectively). U0126 treatment also significantly reduced FK228-induced and H-Ras-induced ROS elevation (Fig. 4b-2) and FK228-induced caspase activation (Fig. 4b-3) and cell death (Fig. 4b-4). Accordingly, Mek1/2 mediated signals to Nox-1 elevation, and these signals were induced by both H-Ras and FK228 treatment. Inhibition of Mek1/2 activity blocked FK228-induced Nox-1 elevation, ROS production, caspase activation, and cell death, indicating a pro-apoptotic role of Mek1/2 in FK228-induced cell death. It is noteworthy that FK228 treatment increased Mek1/2 activity, bypassing the downregulated, upstream regulator Raf-1, to induce Nox-1 elevation leading to ROS production for inducing differential cell death in oncogenic H-Ras-expressing cells versus counterpart cells. In particular, FK228 treatment is able to destabilize Raf proteins through the dissociation of Raf proteins from heat shock protein 70 [18]. Thus, the dual abilities of FK228 to downregulate Raf proteins and to upregulate Mek activity for Nox-1 elevation may constitute the unique property of FK228 to induce selective cell death for controlling oncogenic Ras-expressing cells. Considering the increased Nox-1 level in oncogenic H-Ras-expressing cells, in which a high level of Nox-1 may play a pro-apoptotic role in enhancing ROS production for FK228-induced caspase activation and cell death, we suggest that FK228 should be seriously considered in clinical studies to target cancer cells acquiring oncogenic Ras activation.

Induction of the ERK pathway by FK228-induced mitochondrial reactive oxygen species in 10T1/2 cells

In our earlier report [7], we showed that the treatment of cells with the mitochondrial ROS blocker, ROT [19,20], inhibits FK228-induced cell death of human urinary bladder cancer J82 cells, suggesting a role of mitochondria-produced ROS in FK228-induced cell death. ROS has been shown to stimulate Erk1/2 [21]. To understand the mechanisms underlying the synergistic induction of the ERK pathway and cell death by H-Ras and FK228, we investigated whether mitochondria-produced ROS was induced by FK228 to induce the ERK pathway. We studied the effects of FK228 on the induction of mitochondrial membrane damage, production of mitochondrial ROS, cell death, and the ERK pathway in 10T1/2-TR-H-*Ras* cells. We labeled cells with Rho-123 and

Copyright © Lippincott Williams & Wilkins. Unauthorized reproduction of this article is prohibited.

Fig. 6

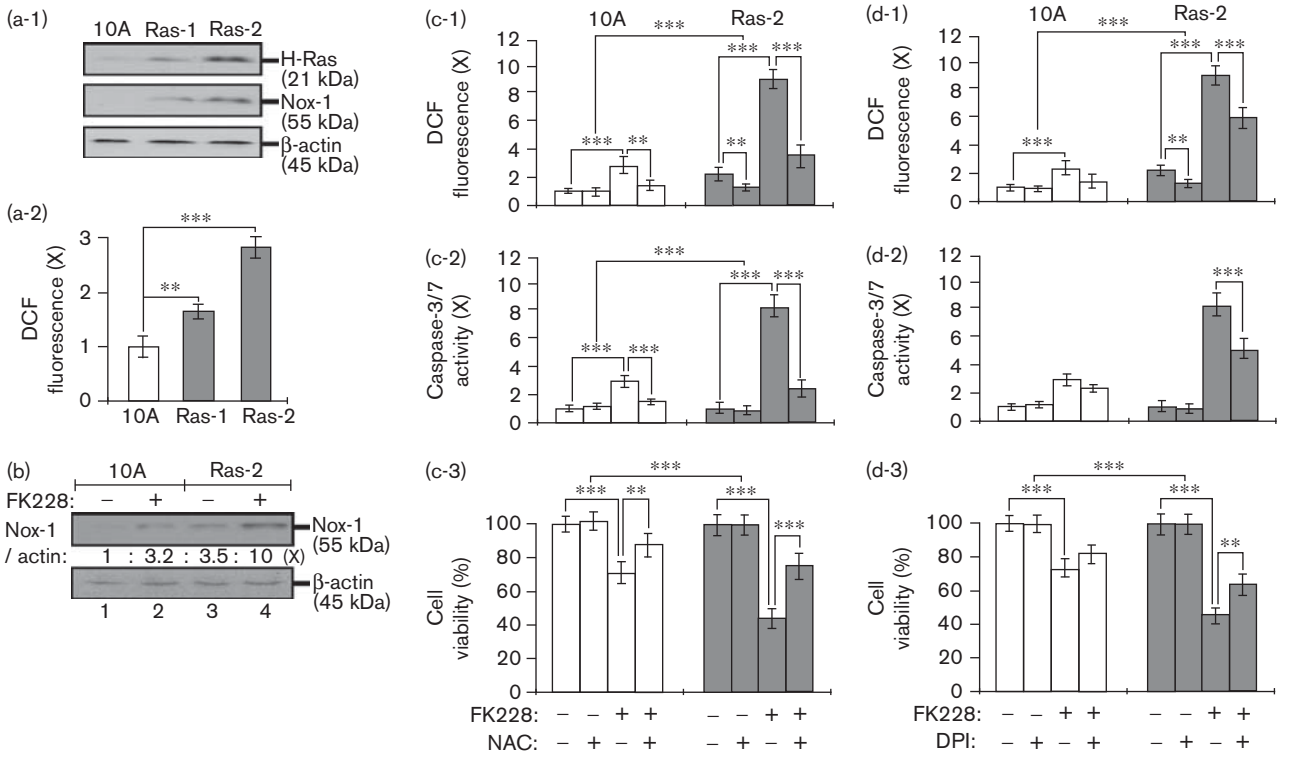

FK228-induced reactive oxygen species (ROS), nicotinamide adenine dinucleotide phosphate-oxidase 1 (Nox-1), and cell death in oncogenic H-Ras-expressing MCF10A cells. (a-1) Cell lysates of MCF10A and oncogenic H-Ras-expressing, MCF10A-Ras-1 and -Ras-2 cells were analyzed by western immunoblotting to detect H-Ras and Nox-1 with β-actin as a control. (a-2) ROS levels were measured; relative level in oncogenic H-Ras-expressing MCF10A cells, as fold induction (X, arbitrary unit), was normalized by the level determined in the parental MCF10A cells, set as 1. (b) MCF10A and MCF10A-Ras-2 cells were treated with 0.5 nmol/l FK228 for 48 h. Cell lysates were analyzed by western immunoblotting to detect Nox-1 with β-actin as a control. Levels of Nox-1 and β-actin were quantified by densitometry. The relative protein levels of Nox-1 (Nox-1/actin) were calculated by normalizing the levels of Nox-1 with the levels of β-actin, and then were normalized by the level in parental MCF10A cells (lane 1), set as 1 (X, arbitrary unit). (c-1–c-3 and d-1–d-3) MCF10A and MCF10A-Ras-2 cells were treated with 0.5 nmol/l FK228 in the presence and absence of 5 nmol/l N-acetyl-L-cysteine (NAC) (c-1–c-3) or 0.1 μmol/l diphenylene iodonium (DPI) (d-1–d-3) for 48 h. (c-1 and d-1) ROS levels were measured; relative level, as fold induction (X, arbitrary unit), was normalized by the level determined in the untreated MCF10A counterpart cells, set as 1. (c-2 and d-2) The activity of caspase-3/7 was measured; relative caspase activity, as fold induction (X, arbitrary unit), was normalized by the value determined in the untreated counterpart cells, set as 1. (c-3 and d-3) Cell viability was determined; relative cell viability was normalized by the value determined in untreated counterpart cells, set as 100%. Columns, mean of triplicates (a-2, c-1, c-2, d-1, and d-2) or tetraplicates (c-3 and d-3); bars, standard deviation. The Student's *t*-test was used to analyze statistical significance, indicated by $^{**}P<0.01$, $^{***}P<0.001$. All results are representative of three independent experiments. DCF, dichlorofluorescein.

found that FK228 treatment induced reduction of mitochondrial membrane potential down to approximately 70 and 90% in oncogenic H-Ras-expressing cells versus counterpart cells, respectively (Fig. 5a), indicating that FK228 treatment induced mitochondrial membrane damage to a higher degree in oncogenic H-Ras-expressing cells than in counterpart cells. Using ROT to block mitochondrial ROS, we found that ROT treatment significantly reduced FK228-increased ROS (Fig. 5b-1), FK228-decreased cell viability (Fig. 5b-2), and FK228-induced phosphorylation of Erk1/2 (Fig. 5b-3) to higher degrees in oncogenic H-Ras-expressing cells than in counterpart cells, indicating that differential induction of mitochondrial ROS was involved in FK228-induced differential cell death and activation of the ERK pathway in oncogenic H-Ras-expressing cells versus counterpart cells. Possibly, differential induction of mitochondrial ROS is one of the mechanisms underlying synergistic induction of the ERK pathway and cell death by H-Ras and FK228. However, the mechanism behind the induction of the ERK pathway by mitochondrial ROS remains to be studied.

The ERK pathway mediated H-Ras-induced and FK228-induced Nox-1, reactive oxygen species, caspase activation, and cell death in MCF10A cells

To address whether differential induction of Nox-1 expression, ROS production, and caspase activation involved in FK228-induced selective cell death of oncogenic H-Ras-expressing cells versus counterpart cells are limited to 10T1/2-TR-H-*Ras* cells, we introduced oncogenic H-Ras into human breast epithelial MCF10A cells. We used an earlier constructed pcDNA4/TO-E-H-*Ras* plasmid [22], which carries the oncogenic H-*Ras* (V12) gene to transfect MCF10A cells and selected stably oncogenic

Copyright © Lippincott Williams & Wilkins. Unauthorized reproduction of this article is prohibited.

Fig. 7

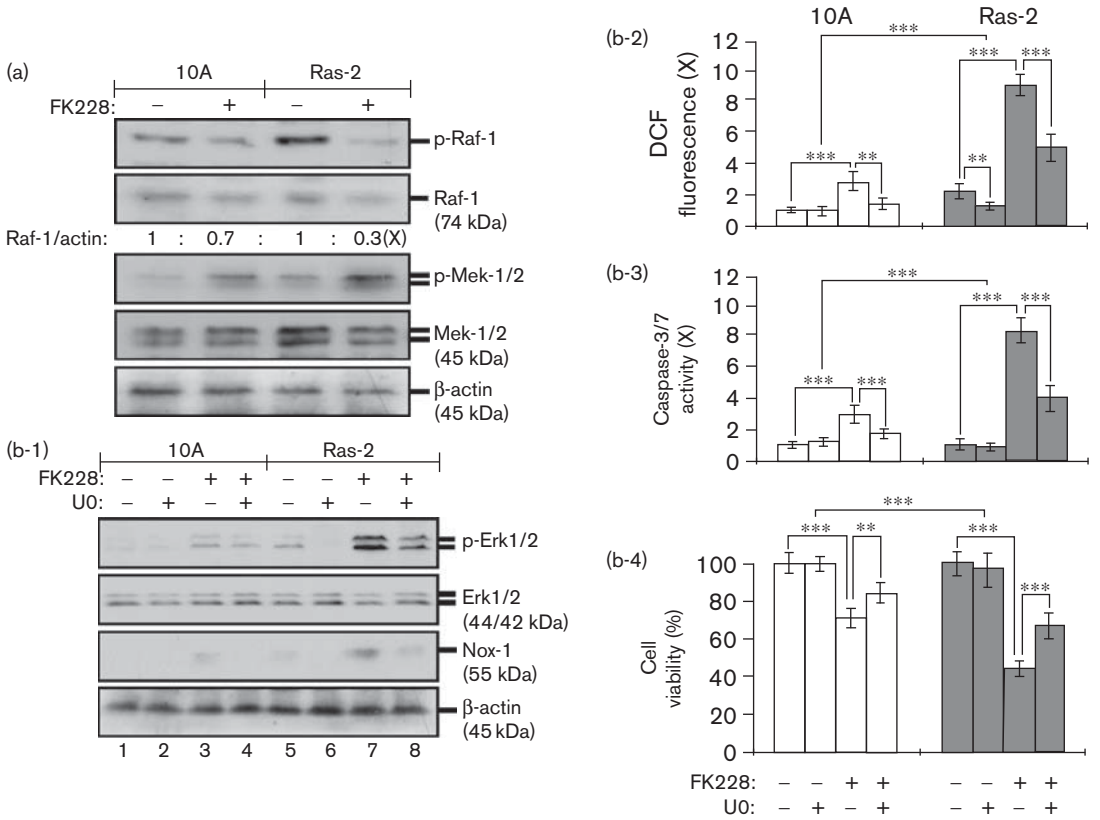

The ERK pathway mediated H-Ras-induced and FK228-induced reactive oxygen species, nicotinamide adenine dinucleotide phosphate-oxidase 1 (Nox-1), and death in MCF10A cells. MCF10A and MCF10A-Ras-2 cells were treated with 0.5 nmol/l FK228 (a, b-1–b-4) in the presence and absence of 10 μmol/l U0126 (U0) (b-1–b-4) for 48 h. (a and b-1) Cell lysates were analyzed by western immunoblotting to detect p-Raf-1, Raf-1, p-Mek1/2, Mek1/2, p-Erk1/2, Erk1/2, and Nox-1 with β-actin as a control. Levels of Raf-1 and β-actin were quantified by densitometry. The relative protein levels of Raf-1 (Raf-1/actin) were calculated by normalizing the levels of Raf-1 with the levels of β-actin, and then were normalized by the level in untreated cells (lane 1), set as 1 (X, arbitrary unit). (b-2) Reactive oxygen species levels were measured; relative level, as fold induction (X, arbitrary unit), was normalized by the level determined in the uninduced, untreated counterpart cells, set as 1. (b-3) The activity of caspase-3/7 was measured; relative caspase activity, as fold induction (X, arbitrary unit), was normalized by the value determined in untreated counterpart cells, set as 1. (b-4) Cell viability was determined; relative cell viability was normalized by the value determined in untreated counterpart cells, set as 100%. Columns, mean of triplicates (b-2 and b-3) or tetraplicates (b-4); bars, standard deviation. The Student's *t*-test was used to analyze statistical significance, indicated by $^{**}P<0.01$, $^{***}P<0.001$. All results are representative of two independent experiments. DCF, dichlorofluorescein.

H-Ras-expressing cell clones. As shown in Fig. 6a-1, MCF10A-Ras-1 and MCF10A-Ras-2 cells (lanes 2 and 3) expressed levels of oncogenic H-Ras distinguishable from the counterpart level in the parental cells (lane 1). In concert with the levels of oncogenic H-Ras, higher levels of Nox-1 (Fig. 6a-1) and ROS (Fig. 6a-2) were detected in MCF10A-Ras-1 and MCF10A-Ras-2 cells than in MCF10A cells. The treatment of cells with FK228 increased Nox-1 level (Fig. 6b), ROS production (Fig. 6c-1 and d-1), caspase activation (Fig. 6c-2 and d-2), and cell death (Fig. 6c-3 and d-3) in both MCF10A and oncogenic H-Ras-expressing MCF10A-Ras-2 cells. Higher degrees of Nox-1 level, ROS production, caspase activation, and cell death were induced by FK228 in MCF10A-Ras-2 cells than in MCF10A cells. Using NAC to block ROS (Fig. 6c-1 to c-3), we found that FK228-induced ROS production (Fig. 6c-1), caspase activation (Fig. 6c-2), and cell death (Fig. 6c-3) were significantly reduced in MCF10A and MCF10A-Ras-2 cells. Using DPI to inhibit Nox-1 (Fig. 6d-1 to d-3), we found that FK228-induced ROS production (Fig. 6d-1), caspase activation (Fig. 6d-2), and cell death (Fig. 6d-3) were significantly reduced in MCF10A-Ras-2 cells. DPI treatment induced a modest reduction of FK228-induced ROS production, caspase activation, and cell death in MCF10A cells. These results indicate that differentially increased Nox-1 played a pro-apoptotic role in FK228-induced differential ROS production, caspase activation, and cell death in oncogenic H-Ras-expressing, human epithelial MCF10A-Ras-2 cells versus counterpart MCF10A cells.

Investigating the role of the ERK pathway in FK228-induced Nox-1 elevation, ROS production, caspase activation, and death of MCF10A and MCF10A-Ras-2 cells, we found that FK228 treatment resulted in reducing phosphorylation of Raf-1 and cognate Raf-1 protein but

Copyright © Lippincott Williams & Wilkins. Unauthorized reproduction of this article is prohibited.

increasing Mek1/2 phosphorylation (Fig. 7a). Inhibition of Mek1/2 activity by U0126 resulted in blocking FK228-induced and H-Ras-induced Erk1/2 phosphorylation and Nox-1 elevation (Fig. 7b-1, lanes 4, 6, and 8 versus lanes 3, 5, and 7, respectively). U0126 treatment also significantly reduced FK228-induced and H-Ras-induced ROS elevation (Fig. 7b-2), FK228-induced caspase activation (Fig. 7b-3) and cell death (Fig. 7b-4). These results were consistent with the findings in 10T1/2-TR-H-*Ras* cells (Figs 2, 3, and 4); differentially increased Nox-1 through the ERK pathway played a pro-apoptotic role in FK228-induced differential ROS production, caspase activation, and cell death in oncogenic H-Ras-expressing, human epithelial MCF10A-*Ras*-2 cells versus counterpart MCF10A cells, in addition to mouse fibroblast 10T1/2-TR-H-*Ras* cells.

Conclusion

In this paper, we showed that Mek1/2 mediated signals from both H-Ras and FK228 treatment to induce Nox-1 elevation for ROS production in both human epithelial MCF10A and mouse fibroblast 10T1/2 cells. Oncogenic H-Ras expression and FK228 treatment synergistically induced Mek1/2 and Erk1/2 activation, bypassing Raf, resulting in differentially increased Nox-1, ROS production, GSH depletion, and caspase activation. These changes led to selective cell death in oncogenic H-Ras-expressing cells versus counterpart cells. FK228 also differentially induced mitochondrial ROS participation to induce the ERK pathway in the selective cell death of oncogenic H-Ras-expressing cells versus counterpart cells. Earlier, we showed that differentially increased intracellular ROS plays an important role in FK228-induced selective apoptosis and differential activation of caspases in oncogenic H-Ras-expressing, human cancer J82-Ras and HT29-Ras versus parental counterpart J82 and HT29 cells, respectively [7]. The high levels of ROS frequently found in cancer cells have been postulated to be incompatible for cell survival and may potentiate cancer cells to be more susceptible to ROS-induced cell death than normal counterpart cells [23]. Thus, targeting the downstream ERK pathway by enhancing the activation of Mek1/2 and Erk1/2 to induce Nox-1 elevation for ROS production and selective cell death should be seriously considered in designing therapeutic protocols targeting cancer cells by ROS-mediated mechanisms using FK228 in combination with other agents. This method may increase the effectiveness of target therapies for treating cancer cells acquiring Ras activation.

Acknowledgements

The author's thank Dr K.K. Chan at the Ohio State University for providing FK228 (National Cancer Institute, Chemistry and Synthesis Branch); D.J. Trent for technique support in flow cytometric analysis of ROS contents and cell death; and M. Bailey for textual editing of the manuscript. This research was supported by the University of Tennessee, College of Veterinary Medicine, Center of Excellence in Livestock Diseases and Human Health (to H.C.R.W.).

References

1 Bos JL. Ras oncogenes in human cancer: a review. *Cancer Res* 1989; **49**:4682–4689.
2 Choudhary S, Wang HCR. Proapoptotic ability of oncogenic H-Ras to facilitate apoptosis induced by histone deacetylase inhibitors in human cancer cells. *Mol Cancer Ther* 2007; **6**:1099–1111.
3 Choudhary S, Wang HCR. Pro-apoptotic activity of oncogenic H-Ras for histone deacetylase inhibitor to induce apoptosis of human cancer HT29 cells. *J Cancer Res Clin Oncol* 2007; **133**:725–739.
4 Fecteau KA, Mei J, Wang HCR. Differential modulation of signaling pathways and apoptosis of Ras-transformed cells by a depsipeptide FK228. *J Pharmacol Exp Ther* 2002; **300**:890–899.
5 Song P, Wei J, Wang HCR. Distinct roles of the ERK pathway in modulating apoptosis of Ras-transformed and non-transformed cells induced by anticancer agent FK228. *FEBS Lett* 2005; **579**:90–94.
6 Konstantinopoulos PA, Vandoros GP, Papavassiliou AG. FK228 (depsipeptide): a HDAC inhibitor with pleiotropic antitumor activities. *Cancer Chemother Pharmacol* 2006; **58**:711–715.
7 Choudhary S, Wang HCR. Role of reactive oxygen species in proapoptotic ability of oncogenic H-Ras to increase human bladder cancer cell susceptibility to histone deacetylase inhibitor for caspase induction. *J Cancer Res Clin Oncol* 2009; **135**:1601–1613.
8 Mitsushita J, Lambeth JD, Kamata T. The superoxide-generating oxidase Nox1 is functionally required for Ras oncogene transformation. *Cancer Res* 2004; **64**:3580–3585.
9 Adachi Y, Shibai Y, Mitsushita J, Shang WH, Hirose K, Kamata T. Oncogenic Ras upregulates NADPH oxidase 1 gene expression through MEK–ERK-dependent phosphorylation of GATA-6. *Oncogene* 2008; **27**:4921–4932.
10 Kamata T. Roles of Nox-1 and other Nox isoforms in cancer development. *Cancer Sci* 2009; **100**:1382–1388.
11 Soule HD, Maloney TM, Wolman SR, Peterson WD Jr, Brenz R, McGrath CM, *et al.* Isolation and characterization of a spontaneously immortalized human breast epithelial cell line, MCF-10. *Cancer Res* 1990; **50**:6075–6086.
12 Trachootham D, Zhou Y, Zhang H, Demizu Y, Chen Z, Pelicano H, *et al.* Selective killing of oncogenically transformed cells through a ROS-mediated mechanism by β-phenylethyl isothiocyanate. *Cancer Cell* 2006; **10**:241–252.
13 Riganti C, Gazzano E, Polimeni M, Costamagna C, Bosia A, Ghigo D. Diphenylene iodonium inhibits the cell redox metabolism and induces oxidative stress. *J Biol Chem* 2004; **279**:47726–47731.
14 Deneke SM. Thiol based antioxidant. *Curr Top Cell Regul* 2000; **36**:151–180.
15 Ballatori N, Krance SM, Notenboom S, Shi S, Tieu K, Hammond CL. Glutathione dysregulation and the etiology and progression of human diseases. *Biol Chem* 2009; **390**:191–214.
16 Chuang JI, Chang TY, Liu HS. Glutathione depletion-induced apoptosis of H-Ras-transformed NIH3T3 cells can be prevented by melatonin. *Oncogene* 2003; **22**:1349–1357.
17 Cagnol S, Chambard JC. ERK and cell death: mechanisms of ERK-induced cell death – apoptosis, autophagy and senescence. *FEBS J* 2010; **277**:2–21.
18 Wang Y, Wang SY, Zhang XH, Zhao M, Hou CM, Xu YJ, *et al.* FK228 inhibits Hsp90 chaperone function in K562 cells via hyperacetylation of Hsp70. *Biochem Biophys Res Commun* 2007; **356**:998–1003.
19 Barrientos A, Moraes CT. Titrating the effects of mitochondrial complex I impairment in the cell physiology. *J Biol Chem* 1999; **274**:16188–16197.
20 Benard G, Bellance N, James D, Parrone P, Fernandez H, Letellier T, *et al.* Mitochondrial bioenergetics and structural network organization. *J Cell Sci* 2007; **120**:838–848.
21 Guyton KZ, Liu Y, Gorospe M, Xu Q, Holbrook NJ. Activation of mitogen-activated protein kinase by H2O2. Role in cell survival following oxidant injury. *J Biol Chem* 1996; **271**:4138–4142.
22 Song P, Wang HCR. Efficient identification of tetR-expressing cell lines for tetracyline-regulated gene expression. *Electron J Biotechnol* 2004; **7**:210–213.
23 López-Lázaro M. Dual role of hydrogen peroxide in cancer: possible relevance to cancer chemoprevention and therapy. *Cancer Lett* 2007; **252**:1–8.

Copyright © Lippincott Williams & Wilkins. Unauthorized reproduction of this article is prohibited.